Chemosphere 283 (2021) 131219

Contents lists available at ScienceDirect

Chemosphere

journal homepage: www.elsevier.com/locate/chemosphere

Effects of different fluid fields on the formation of cyanobacterial blooms

Peng Gu [a], Guoping Zhang [c], Xin Luo [a], Lianghao Xu [c], Weizhen Zhang [a,b,*], Qi Li [a], Yuyang Sun [d], Zheng Zheng [a,**]

[a] Department of Environmental Science and Engineering, Fudan University, Shanghai, China
[b] School of Ecological Environment, Chengdu University of Technology, Chengdu, China
[c] China Ship Scientific Research Center, Wuxi, China
[d] Phillips Exeter Academy '20 graduate', Exeter, NH, USA

ARTICLE INFO

Handling Editor: Tsair-Fuh

Keywords:
Cyanobacterial bloom
Fluid field
Shear stress
Growth
Buoyancy

ABSTRACT

Cyanobacterial blooms have been attracting more and more attention, and the mechanism is widely studied. However, the effects of fluid fields on the bloom formation were rarely reported. In this study, the effects of fluid fields formed under different external conditions were investigated. The results indicated that low wind speed (3 m/s) was conducive to the formation of cyanobacterial blooms, while high wind speed (6 m/s) was adverse. For low wind speed, an upward fluid field was detected by particle image velocimetry. This fluid field accelerated the algal growth by 58.6%, and improved the buoyancy by up-regulating the genes involved in the synthesis of gas vesicles and extracellular polymeric substances. In addition, the boundary shear stress induced the colony formation of cyanobacteria and improved the aggregation proportion significantly ($p < 0.05$), which was beneficial to bloom formation. As a result, cyanobacterial blooms are more likely to form on the lake shore under moderate breeze. When wind speed increased to 6 m/s, a downward fluid field was formed, causing algal cells to gather at the bottom and hindering the bloom formation. These results provided a theoretical basis for field researches related to the formation of cyanobacterial blooms and the treatment of cyanobacteria.

1. Introduction

With the rapid population growth and urbanization, many lakes are facing problems of eutrophication, and the cyanobacterial blooms caused by eutrophication have seriously affected the daily life of residents (Qin et al., 2010). Some species of cyanobacteria can produce toxins during metabolism and degradation. For example, *Microcystis* releases liver toxins such as microcystin when it dies, which seriously threatens the safety of drinking water supplies (Pratik et al., 2018). In order to control the harmful cyanobacterial blooms, the most important task is to understand its formation mechanism. Cyanobacterial blooms are defined as a distinct visible discoloration of the water that is primarily caused by cyanobacteria (Huisman et al., 2018), and the key factors for cyanobacterial bloom formation include a large amount of biomass, sufficient buoyancy and suitable hydrodynamic conditions (Qin et al., 2018).

First of all, the formation of cyanobacterial blooms requires the accumulation of huge cyanobacterial biomass in a short time, and the rapid growth of cyanobacteria needs to meet certain environmental conditions. Numerous studies have proved that the main factors affecting the growth of cyanobacteria include temperature, light intensity, nutrient concentration and other trace elements. Researchers have found that 25–30 °C is the most suitable temperature for the growth of cyanobacteria (Imai et al., 2008). When the light intensity reaches 550 Lux, the cyanobacteria can start to multiply rapidly (Krüger and Eloff, 2010). Nutrients are necessary for the growth of cyanobacteria, and the nutrient thresholds are considered to be 0.80 and 0.058 mg/L for total nitrogen and total phosphorus, respectively (Xu et al., 2015). In addition, various metal and liquid ions will affect the growth of cyanobacteria as well (Baptista and Vasconcelos, 2006; Fan et al., 2019b). However, the effects of fluid fields on the growth of cyanobacteria are still rarely reported. Some studies have pointed out that the flow rate could affect the growth of cyanobacteria (Acuña et al., 2011; Mitrovic et al., 2011; Zhou et al., 2016b), but the mechanism analysis was scarce.

The buoyancy of algal cells is also one of the important factors for the

* Corresponding author. Department of Environmental Science and Engineering, Fudan University, Shanghai, China.
** Corresponding author.
E-mail addresses: zhangwz15@fudan.edu.cn (W. Zhang), zzhenghj@fudan.edu.cn (Z. Zheng).

https://doi.org/10.1016/j.chemosphere.2021.131219
Received 10 January 2021; Received in revised form 31 May 2021; Accepted 10 June 2021
Available online 15 June 2021

formation of cyanobacterial blooms, and its main sources include the intracellular gas vesicles and the colonies formed between cells (Reynolds et al., 1987). Gas vesicle is a prismatic cavity with a diameter of 75 nm. The main component of the outer wall is protein, and the inside is gas (Bowen and Jensen, 1965). The number of gas vesicle in bloom-formed algal cells can reach more than 100 times that of algae cells cultured in the laboratory. Apart from gas vesicles, the formation of colonies can also provide extra buoyancy (Zhang et al., 2011). Under the stimulation of external conditions, algal cells can secrete extracellular polymeric substances (EPS), which promotes the formation of colonies (Chen et al., 2019). It is reported that high concentration of calcium ions can encourage the secretion of EPS of algal cells, thereby increasing the aggregation proportion of cells and obtaining a higher floating rate (Gu et al., 2020). Besides, the grazing of zooplankton such as flagellates will also cause colony formation of algal cells and lead to a higher buoyancy (Yang et al., 2010). Although there have been some studies on the factors affecting the buoyancy of algal cells, the research on the fluid field is still very limited.

Finally, suitable fluid field conditions can promote the formation of cyanobacterial blooms. Numerous field studies have found that there are similar hydrodynamic and wind characteristics during cyanobacterial blooms. Through long-term observations of Lake Taihu, it is found that breeze (wind speed <3 m/s) is beneficial to the formation of cyanobacterial blooms (Wang et al., 2010). Field study found that the distribution of cyanobacteria in Lake Taihu before and after the typhoon passed by was significantly different (Qin et al., 2016). When the typhoon passed, the average wind speed rose to 6–8 m/s, and the algal cells were evenly distributed in the water column. After the typhoon, the wind speed decreased to 2 m/s, which caused an upward water flow in vertical direction and accelerated the floating of algal cells. Three-month researches of Lake Tiefer See in Germany have reached similar conclusions, and cyanobacteria was multiplied rapidly under an average wind speed less than 3.5 m/s (Ulrike et al., 2016). Based on these results of field studies, the suitable fluid field conditions for the formation of cyanobacterial blooms can be inferred, however, the mechanism is still unclear and needs to be improved.

Multiple studies have focused on the factors affecting the formation of cyanobacterial blooms. However, researches on the effects of fluid fields are rarely reported. The main difficulty in studying the effect of the fluid field is that it is difficult to describe the fluid field quantitatively. In this study, we investigated the effects of fluid fields from three aspects. First, the fluid fields under different experimental conditions were described by particle image velocimetry (PIV) system. Then, the effects of different fluid fields on the growth of algal cells were estimated using the cell density and enzyme activities. Finally, the buoyancy of algal cells was evaluated by measuring the total EPS contents and the aggregation proportion. Quantitative real-time PCR of specific gene fragments involved in the synthesis of gas vesicles and EPS was implemented to confirm the results of the experiment. The results of this study can provide a theoretical basis for field researches related to the formation of cyanobacterial blooms and the treatment of cyanobacteria.

2. Materials and methods

2.1. Experimental design

Different fluid fields were obtained by using electric fans (wind speeds: 3 m/s and 6 m/s) and wave pumps (flow rate: 0.12 m/s, number of pumps: 2) in this study, and 9 experimental groups were set up (Table 1). The 9 experimental groups involving in the measurements of fluid fields were conducted on the same day. For each measurement, the fluid field was continuously measured for 2–3 min after the system was stable. The flow velocity obtained of the fluid field was the average over 2–3 min, therefore, no replicate was set as the external conditions were unchanged. Transparent acrylic reactors with a total volume of 150 L (50 × 50 × 60 cm) were used. The *Microcystis aeruginosa* (FACHB-912) used in this study was purchased from the Institute of Hydrobiology, Chinese Academy of Sciences (Wuhan, China), and the initial cell density was controlled at 2×10^5 cells/mL. During the experiment, *M. aeruginosa* was cultured in BG-11 medium (Rippka et al., 1979) under controlled conditions at 28 ± 2 °C with a light intensity of 1500 lx (12 h light/12 h dark cycle), and a relative humidity of 70–90% (Jiang and Zheng, 2018). The duration of this study was 10 days. At the beginning of the experiment, the initial liquid level was marked on the reactor. Distilled water was replenished every 2 days until the liquid level was the same as the initial to ensure that the total volume of each reactor was unchanged. The cell density was then detected to avoid errors caused by volume changes.

Table 1
Experimental group settings and maximum, minimum and average values of shear stress in different fluid fields.

No.	Wind Speed (m/s)	Number of wave pumps	Max. (Pa)	Min. (Pa)	Ave. (Pa)
1	0	0	4.47×10^{-4}	4.99×10^{-9}	3.93×10^{-5}
2	0	1	5.08×10^{-3}	1.78×10^{-7}	7.41×10^{-4}
3	0	2	4.58×10^{-3}	8.73×10^{-8}	9.39×10^{-4}
4	3	0	1.25×10^{-3}	9.70×10^{-9}	5.82×10^{-5}
5	3	1	5.12×10^{-3}	2.75×10^{-7}	7.70×10^{-4}
6	3	2	5.60×10^{-3}	1.43×10^{-7}	9.48×10^{-4}
7	6	0	2.14×10^{-3}	3.60×10^{-8}	7.35×10^{-5}
8	6	1	4.36×10^{-3}	1.15×10^{-7}	8.03×10^{-4}
9	6	2	5.02×10^{-3}	4.40×10^{-7}	9.56×10^{-4}

2.2. Fluid fields and shear stress

The fluid fields under different hydrodynamic conditions were measured by PIV system (TSI, USA). PIV consists of three parts: laser source, CCD camera and analysis software (Fig. S1). Pulsed laser (NewWave, USA) is used as the laser source with a maximum output power of 200 mJ per pulse. The wavelength of pulsed laser is 532 nm, and the duration of each pulse is about 10 ns. The image is collected using a 4 M pixel high-resolution CCD camera (TSI, USA). The measurement area of PIV is about 420 × 360 mm and the spatial resolution is 7.5 mm, that is, a total of 56 × 48 = 2688 data points per test plane. The acquired images are processed by cross-correlation to obtain the velocity vector (u, v) in the horizontal and vertical directions at the coordinate (x, y), and the fluid field of the plane is drawn accordingly. In this study, the plane facing the wave pump was defined as the front, and the fluid fields of 4 planes (F1: front, 5 cm from the wall; F2: front, 25 cm from the wall; S1: side, 5 cm from the wall; S2: side, 25 cm from the wall) were detected.

After obtaining the velocity vector measured by PIV, the shear stress at the corresponding position can be calculated by the following formula (Liu et al., 2006):

$$\tau i,j = \mu\left(\frac{u_{x\,i,\,j+1} - u_{x\,i,j-1}}{y_{i,\,j+1} - y_{i,j-1}} + \frac{v_{y\,i+1,\,j} - v_{y\,i-1,j}}{x_{i+1,\,j} - x_{i-1,j}}\right) \quad (2\text{-}1)$$

where ux and vy are the velocity in the x and y directions, respectively; i and j are used to determine the position in the x and y directions, and their value ranges are 1–56 and 1–48, respectively. In this study, the data measured by PIV was calculated using a self-written program made in Python language to obtain the shear stress of each experimental group.

2.3. Algal growth and spatial distribution

To investigate the algal growth of each group, cell densities were measured after 2, 4, 6, 8 and 10 days. Meanwhile, samples were collected at 9 positions (upper, middle, and lower parts of the reactor) to analyze the spatial distribution and aggregation proportion of algae cells on the 10th day. To ensure the accuracy of the position during the collection of samples, two operations were used. First, as the reactors were made of transparent acrylic, a black marker was used to make grid divisions on the outside of the reactor. Second, the pipette used in the experiment was also marked at specific heights corresponding to the sampling positions. 1 mL of algal sample was pipetted into a centrifuge tube and fixed with 10 μL of Lugol's reagent. Cell density was determined using an automatic algae counter (Countstar® BioMarine, ALIT Life Science, China) (Zheng et al., 2020). The aggregation proportion was calculated as follows:

$$\text{Aggregation Proportion} = \frac{\textit{Colonial Algal Cell Number}}{\textit{Total Algal Cell Number}} \quad (2\text{-}2)$$

Where the number of single algal cell was counted directly by the algae counter, and colonial cell numbers were calculated automatically according to the pre-set parameters, including diameter, roundness, brightness, etc. Each sample was counted 5 times and averaged after removing the maximum and minimum values.

2.4. Total EPS contents

EPS can be divided into dissolved EPS and bound EPS, in this study, the sum of the two types of EPS was detected. The main components of EPS are polysaccharides, proteins, lipids, DNA, etc., among them, the contents of polysaccharides and proteins were investigated in this study. 15 mL of each sample was ultrasonicated (SB-3200D, SCIENTZ, China) at 150 W for 30 s and then centrifuged at 3000×*g* for 15 min (VELOCITY 14R, Dynamica, Australia). The supernatant was collected for the measurements of polysaccharides and proteins. The concentration of polysaccharides was analyzed using the phenol-sulfuric acid method (Dubois et al., 1956), while proteins were detected with the bicinchonininc acid (BCA) method (Smith et al., 1985).

2.5. Enzyme activity

In this study, four common antioxidant stress indicators, superoxide dismutase (SOD), catalase (CAT), glutathione (GSH) and malondialdehyde (MDA), were analyzed. 25 mL algal cells of each group were collected on the 10th day, then centrifuged at 3000×*g* for 15 min and the supernatant was removed. The remaining algal cells were transferred into PBS (0.01 M) and homogenized at 12000 r·min^{-1} for 2 min (FSH-2A, Xinrui Instrument., China) to break the cells. Homogenized solution was centrifuged at 12000×*g* for 15 min at 4 °C. The supernatant was used to determine the enzyme activities using assay kits (Nanjing Jiancheng Bioengineering Institute, China) following the manufacturer's instructions.

2.6. Quantitative real-time PCR

RNA extraction. Total RNA was extracted with Trizol reagent (Invitrogen, USA) and treated with RNase-Free DNase I (TaKaRa, Japan) to remove DNA contaminants. The integrity of RNA was confirmed on the Tanon 2500 gel imaging system (Tianneng Company, China) by agarose gel electrophoresis, while RNA concentrations were determined using a NanoDrop 2000 spectrophotometer (Thermo, USA).

First-strand cDNA synthesis. The qualified and quantified total RNA was reverse transcribed into cDNA according to the manufacturer's instructions (PrimeScript™ 1st stand cDNA Synthesis Kit). First, added 600 ng total RNA, 1 μL Oligo(dT) (50 μM) and 1 μL dNTP Mix (10 mmol/L) into the tube in ice bath and added RNase free dH_2O to make a total volume of 10 μL. Then, incubated at 65 °C for 5 min and transferred in ice bath after completion. Next, added 4 μL of buffer, 0.5 μL of RNase inhibitor (40 U/μL) and 1 μL of MMLV RT (200 U/μL) and controlled the volume at 20 μL with RNase free dH_2O. Finally, reacted at 42 °C for 45 min, and completed the reaction by heating at 95 °C for 5 min.

Quantitative real-time PCR. Quantitative real-time PCR was performed to analyze the expression of unigenes. In this study, the expression of 4 genes related to gas vesicle formation (*gvpC*, *gvpG*, *gvpJ*, *gvpK*) (Chen et al., 2019) and 2 genes related to EPS synthesis and transport (*rfbB*, *cpsF*) (Lajwant et al., 1991; Thurlow et al., 2009) in *M. aeruginosa* was validated. Information about specific primers was collected from literature (Table S1) and 16S RNA was used as the internal control. For each PCR reaction, 10 μL SYBR real-time PCR premixture (Vazyme Biotech, China) and 0.4 μL 10 μM forward and reverse primer were added into the tube in ice bath, and diluted to 20 μL with RNase free dH_2O. The amplification cycling program was as follows: 95 °C for 5 min, 40 cycles of 95 °C for 15 s, and 60 °C for 30 s. Quantitative real-time PCR analysis was conducted in triplicate and relative expression was calculated using the $2^{-\Delta\Delta CT}$ method (Schmittgen and Livak, 2008).

2.7. Statistical analysis

Data were analyzed by one-way analysis of variance (ANOVA) and significant differences were determined using Tukey's test, followed by Duncan's test. Statistical analysis was performed using the SPSS 17.0 software (IBM, USA). Each treatment was performed in triplicate and statistical significance was $P < 0.05$.

3. Results

3.1. Fluid fields and shear stress

3.1.1. Fluid fields under different conditions

In this study, the plane facing the wave pump was defined as the front, and the fluid fields of 4 planes (F1: front, 5 cm from the wall; F2: front, 25 cm from the wall; S1: side, 5 cm from the wall; S2: side, 25 cm from the wall) were detected of the 9 experimental groups by PIV system (Fig. 1 and Figs. S2–S4). The flow velocity is calculated by two consecutive images (Fig. S1c). The time interval between the two images taken by the CCD camera is △t. Through the correlation calculation of the two images, the displacement of the particle cluster at each position in the image is determined as △X, and the flow velocity is equal to △X divided by △t. Results showed that the flow velocity was less than 0.003 m/s without the influence of external conditions. The fluid field showed significant differences according to the wind speed. For the wind speed of 3 m/s, the fluid field showed an upward trend and the flow velocity was between 0.003 and 0.008 m/s. When the wind speed increased to 6 m/s, the direction of the fluid field was downward, and the flow velocity was between 0.005 and 0.01 m/s. After adding the wave pumps, the flow velocity increased remarkably with the highest value of 0.1–0.2 m/s. The fluid fields of the groups using wave pumps were similar. Two water streams in opposite directions were formed at the edge of the reactor, and the flow velocity at the boundary was significantly higher than that in the middle (S1 and S2 planes). Meanwhile, it was found that the influence of the wind on the fluid field was weakened and only showed small changes of local flow velocity.

3.1.2. Shear stress of different fluid fields

After measuring the velocity vectors at different positions by PIV system, the shear stress at the corresponding position can be calculated by formula (2-1) (Figs. S5–S8). The average, maximum and minimum values of shear stress in different fluid fields were filtered using a self-written program made in Python language (Table 1). The average shear stress of the control was 3.93 × 10-5 Pa and was randomly

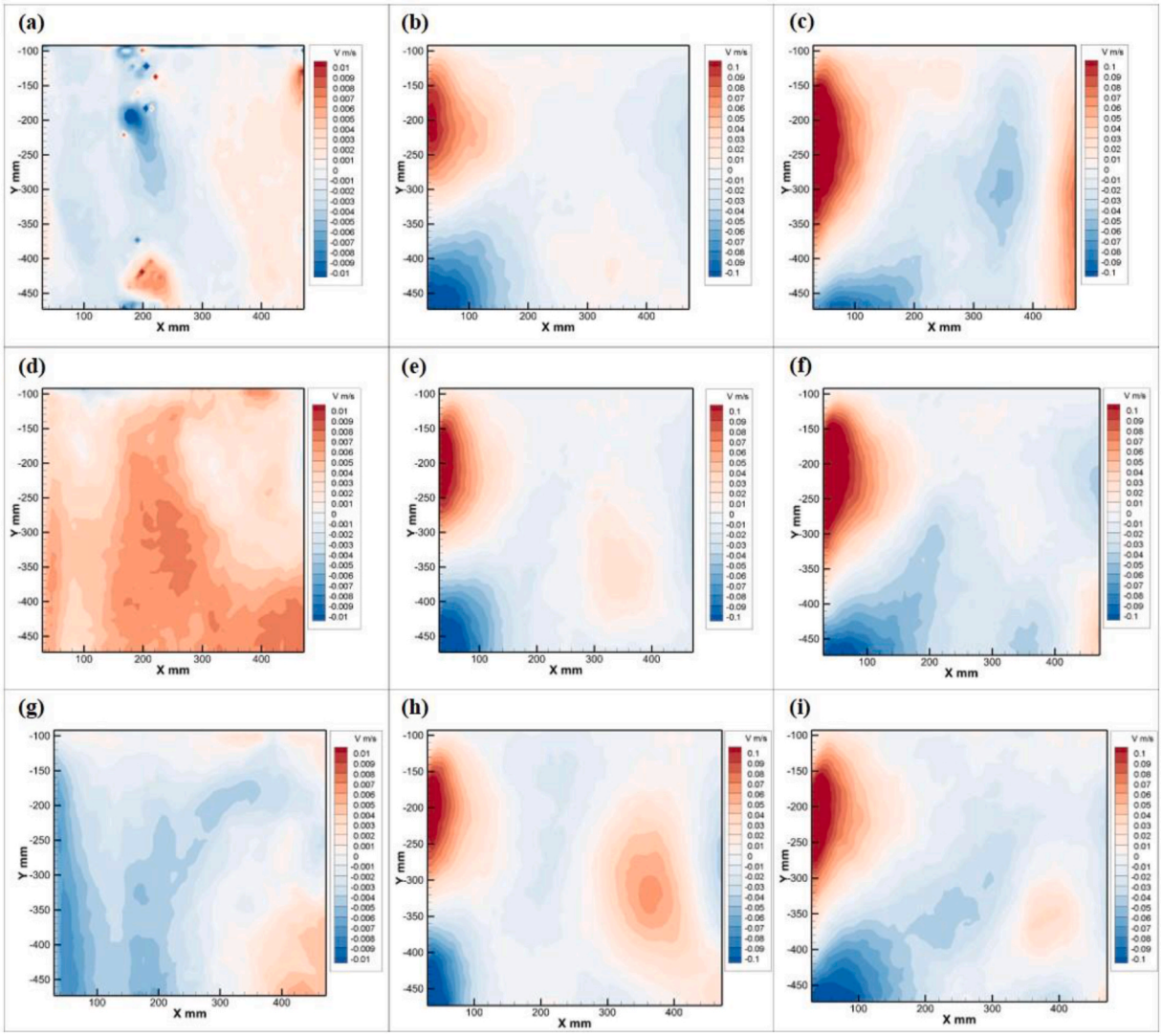

Fig. 1. Vertical velocity distribution diagrams of the S1 plane (the plane on the side of the wave pump was defined as the side, and the S1 plane is 5 cm from the wall). Different colors represent the direction of vertical velocity: upward (red) and downward (blue). The letters (a)–(i) of each diagram represent the experimental groups (1)–(9), respectively. (For interpretation of the references to color in this figure legend, the reader is referred to the Web version of this article.)

distributed. For the group of low wind speed (3 m/s), the shear stress increased to 5.82 × 10-5 Pa, and the shear stress at the bottom boundary increased significantly, with a maximum value of 1.25 × 10-3 Pa. The shear stress of the high wind speed group (6 m/s) further increased, and the average and maximum values were 7.35 × 10-5 Pa and 2.14 × 10-3 Pa, respectively. After the addition of one wave pump, the high shear stress area was concentrated at the exit of the pump, and the average and maximum shear stress were increased by 11 times and 19 times, separately. When two wave pumps were added, the average shear stress increased by 22.9% compared with one wave pump.

According to the results of fluid field measurements, major differences were observed between the groups of different wind speeds and the existence of wave pump, therefore, the fluid fields formed under the conditions of stationary state (Ct), low wind speed (3 m/s, no wave pump) (FF1), high wind speed (6 m/s, no wave pump) (FF2) and one wave pump (no wind, flow rate of 0.12 m/s) (FF3) were selected for subsequent experiments.

3.2. Algal growth analysis

3.2.1. Growth curve

The growth curve of cyanobacteria was estimated by detecting the

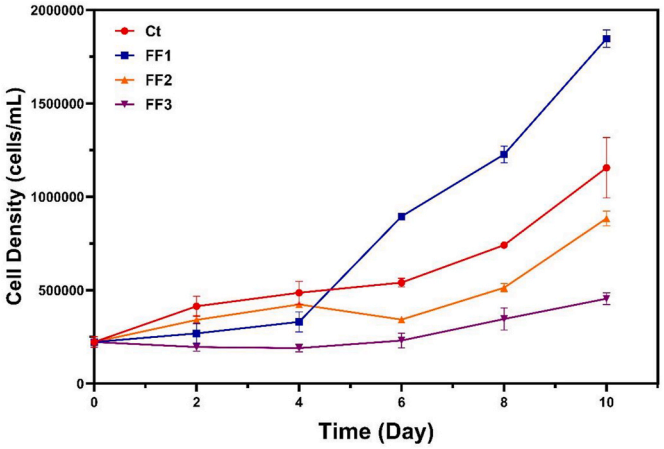

Fig. 2. Growth curves of cyanobacteria under different fluid fields. Ct: Control, FF1: Wind speed 3 m/s, FF2: Wind speed 6 m/s, FF3: One wave pump (flow rate 0.12 m/s). Data are represented as means ± standard deviation analyzed from three replicates.

cell densities (Fig. 2). The results indicated the algal growth of all the groups was slow during the first 4 days. Starting from day 6, the experimental groups entered the logarithmic growth phase. The growth rate of FF1 was significantly higher than that of the other groups; meanwhile, the growth rate of FF2 and FF3 was slower than that of the control. At the end of the experiment, cell density of the control was 1.16×10^6 cells/mL, while the values of FF1, FF2 and FF3 were 1.84×10^6, 8.84×10^5 and 4.54×10^5 cells/mL, respectively.

3.2.2. Antioxidant response

The antioxidant response indicators of algal cells can characterize the extent of cell damage (Fig. S9). In order to explain the mechanism of the effects of fluid fields on the growth of cyanobacteria, four common indicators, including superoxide dismutase (SOD), catalase (CAT), glutathione (GSH) and malondialdehyde (MDA), were analyzed (Fig. 3). Results showed that the anti-oxidative stress-related enzyme activities in the FF3 group were significantly increased ($p < 0.05$). Comparing with the control, the values of SOD, CAT, GSH and MDA increased to 704%, 286%, 139% and 277%, respectively, which revealed that high shear stress (7.41×10^{-4} Pa) can cause serious damage to algal cells. On the contrary, the values of these indicators in the FF1 group were smaller than that of the control.

3.3. Algal buoyancy analysis

3.3.1. Spatial distribution

The spatial distribution of algal cells was analyzed by measuring the cell densities of 9 positions in the reactor (Fig. 4), and it was found that the algal distribution under different fluid fields was significantly different. Algal cells in the control group were mainly accumulated at the bottom of the reactor (47.7%), followed by the upper part (32.7%), and the middle part (19.6%). Algal cells were evenly distributed in the FF1 group, and the cell density in the upper part (35%) was slightly higher than that in the middle (32.8%) and lower parts (32.2%). In the FF2 group, most of the cells gathered in the middle (39.5%) and lower part (35.4%) of the reactor. In the FF3 group, a clear floating layer was observed and the proportion of algal cells in the upper part (53.5%) was higher than that in the middle (25.7%) and lower parts (20.8%).

3.3.2. Quantitative real-time PCR

The spatial distribution of cyanobacteria differed substantially under different fluid fields. In order to explore the causes, 4 genes related to gas vesicle formation (*gvpC*, *gvpG*, *gvpJ*, *gvpK*) and 2 genes related to EPS synthesis and transport (*rfbB*, *cpsF*) were studied by quantitative real-time PCR to determine the expression of related genes (Fig. 5). The results of quantitative real-time PCR indicated that in the FF1 group and FF3 group, the expression of genes related gas vesicle formation was significantly higher than that of the control, while the expression of the FF2 group was the lowest. For the genes related to EPS synthesis and transport, compared with the control group, the FF3 group was remarkably up-regulated, and the FF1 group was down-regulated.

3.3.3. Total EPS contents and aggregation proportion

The expression of genes related to EPS synthesis and transport has been changed significantly under different fluid fields, therefore, the total EPS contents of different experimental groups were subsequently detected (Fig. 6a). The main components of EPS are polysaccharides and protein (Phélippé et al., 2019), which was investigated in this study. Results showed that the proportion of polysaccharides in EPS was a lot higher than that of protein. The content of protein in different groups showed no difference, and the main substance causing differences in EPS was polysaccharides. The total EPS content of each group was consistent with its gene expression level. The control was the same as the FF2 group, the FF1 group was less than the control, and the FF3 group was much higher than the control.

High EPS content can promote the aggregation of algal cells, thereby changing the morphology of colonies and accelerating the floating rate. Thus, the aggregation proportion of algal cells at different positions in the reactor was further analyzed (Fig. 6b). The average aggregation proportion of different experimental groups was highly correlated with its EPS content, meanwhile, considerable differences were observed in different positions of the reactor. The aggregation proportion decreased gradually from higher part to lower part in the reactor of the control, and there was no difference between each position in the FF1 group. In the FF2 group, the aggregation proportion in the medium and lower part was larger than that in the higher part, while in the FF3 group, the higher part was significantly larger than the medium and lower part.

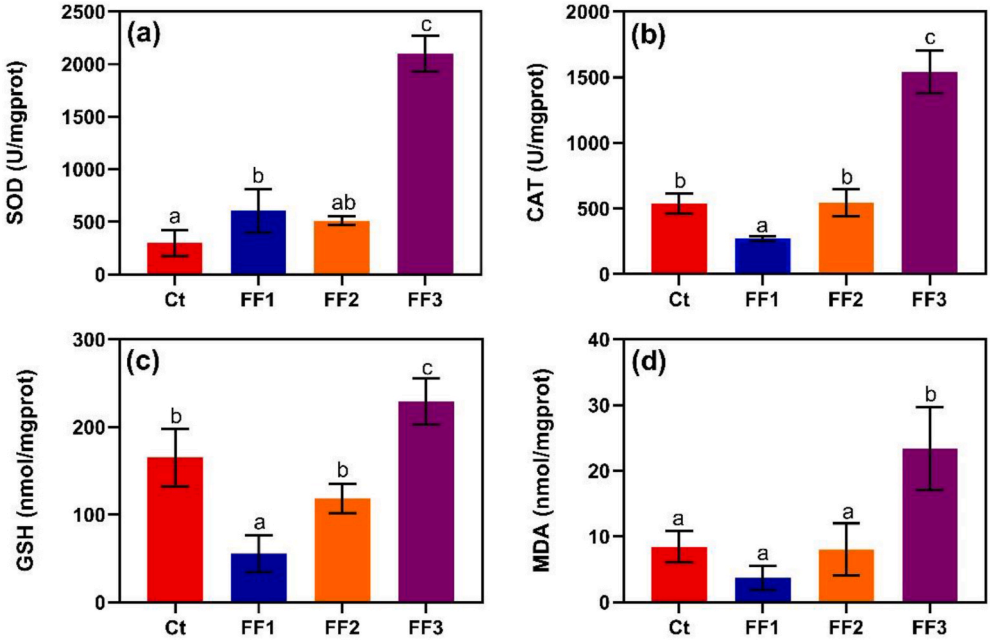

Fig. 3. Antioxidant stress indicators of algal cells under different fluid fields. (a) Superoxide dismutase (SOD), (b) Catalase (CAT), (c) glutathione (GSH), (d) Malondialdehyde (MDA). Ct: Control, FF1: Wind speed 3 m/s, FF2: Wind speed 6 m/s, FF3: One wave pump (flow rate 0.12 m/s). Data are represented as means ± standard deviation analyzed from three replicates. Different characters indicate significant difference ($P < 0.05$; Tukey's test, followed by Duncan's test).

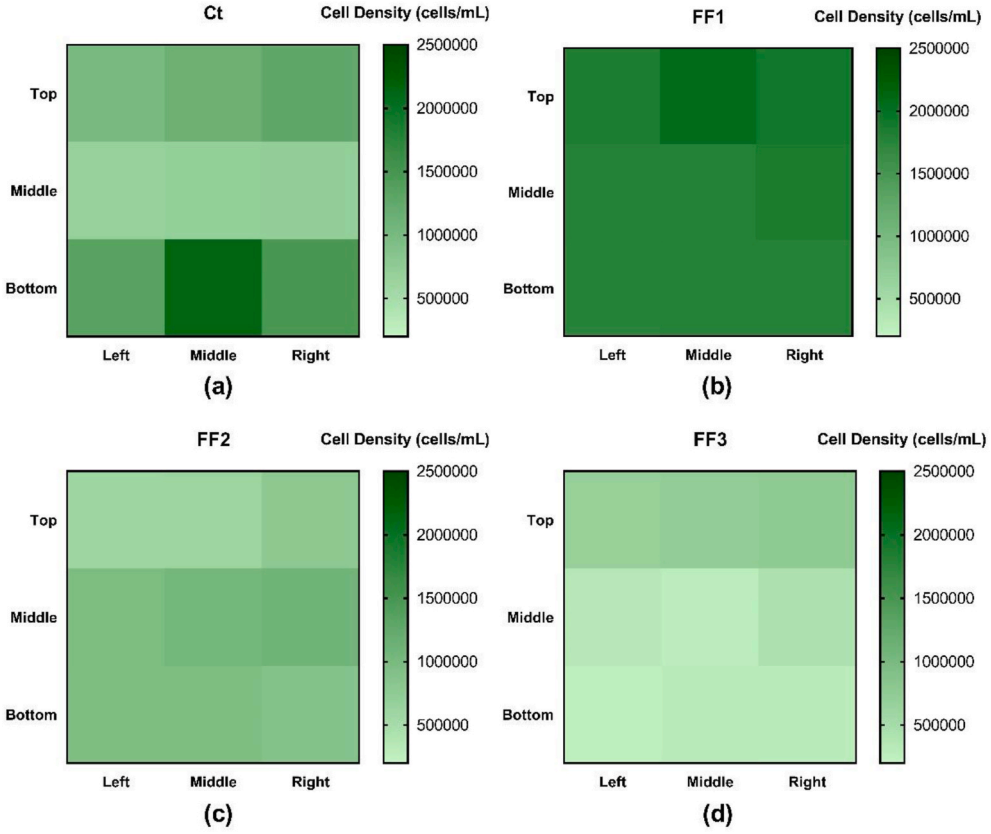

Fig. 4. Spatial distribution heat-map of algal cells in the reactor. Ct: Control, FF1: Wind speed 3 m/s, FF2: Wind speed 6 m/s, FF3: One wave pump (flow rate 0.12 m/s).

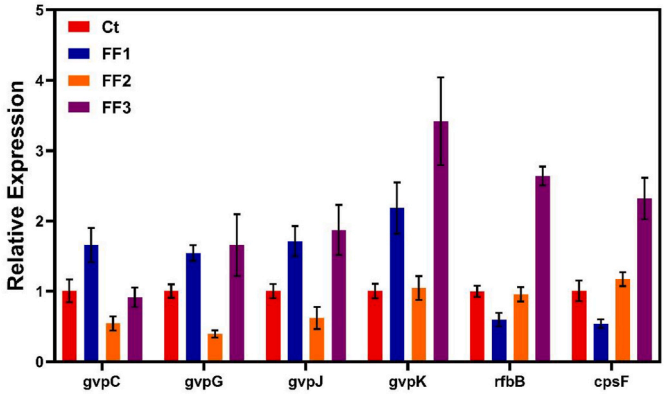

Fig. 5. The expression of related genes determined by quantitative real-time PCR analysis. The expression of the control was set as 1, and the relative expression level was calculated for the following genes: 4 genes related to gas vesicle formation (gvpC, gvpG, gvpJ, gvpK) and 2 genes related to EPS synthesis (rfbB, cpsF). Ct: Control, FF1: Wind speed 3 m/s, FF2: Wind speed 6 m/s, FF3: One wave pump (flow rate 0.12 m/s). Data are represented as means ± standard deviation analyzed from three replicates.

4. Discussion

4.1. Effects of fluid fields on algal growth

The fluid fields showed significant impacts on the growth of cyanobacteria. In this study, the FF1 group promoted the algal growth (Fig. 2), while the growth rate of the FF2 group slowed down. For a stronger fluid field in the FF3 group, the growth of cyanobacteria was significantly inhibited. Previous studies have proved that the flow rate could affect the growth of cyanobacteria (Acuña et al., 2011; Mitrovic et al., 2011; Zhou et al., 2016b) and the trend of algal growth was similar to the results of this study. The algal growth was promoted under low flow rate, as the flow rate increased, the growth rate slowed down gradually. Through the analysis of the vertical distribution of nutrients under the disturbance of different fluid fields, it is found that fluid field can only increase the quantity of suspended solids, but have no obvious effect on the dissolved nutrient contents (Zhu et al., 2004). In this study, BG-11 medium provides sufficient nutrients for algal growth, therefore, it can be inferred that fluid field do not affect the growth by changing the concentration of nutrients, and further analysis is needed to explain the mechanism.

The main effect of the fluid field on algal cells is the shear stress acting on the cell surface. The average shear stress of the control was 3.93×10^{-5} Pa (Table 1), and increased to 5.82×10^{-5} Pa, 7.35×10^{-5} Pa and 7.41×10^{-4} Pa for the 3 experimental groups, respectively. High shear stress can cause the damage on the cell surface of cyanobacteria and induced anti-oxidative stress response. Excessive shear stress can even cause the rupture and death of algal cells (Liang et al., 2013). A former study on submerged plants has also confirmed that high-speed water flow can trigger the antioxidant response on the surface, and the activity of SOD and CAT was amplified (Li et al., 2020). In this study, the antioxidant response of cyanobacteria was analyzed by measuring SOD, CAT, GSH and MDA. It was found that in the FF3 group, the four indicators were significantly increased (Fig. 3), which proved that high shear stress can cause severe damage to algal cells, resulting in the inhibition of algal growth. On the contrary, the antioxidant response indicators in the FF1 group, except for SOD, were conspicuously lower than the control, revealing that the fluid field formed by low wind speed was beneficial to the survival of cyanobacteria. The indicators of the FF2 group showed no difference compared with the control, however, the growth rate of the FF2 group was slower. It was reported that the flow

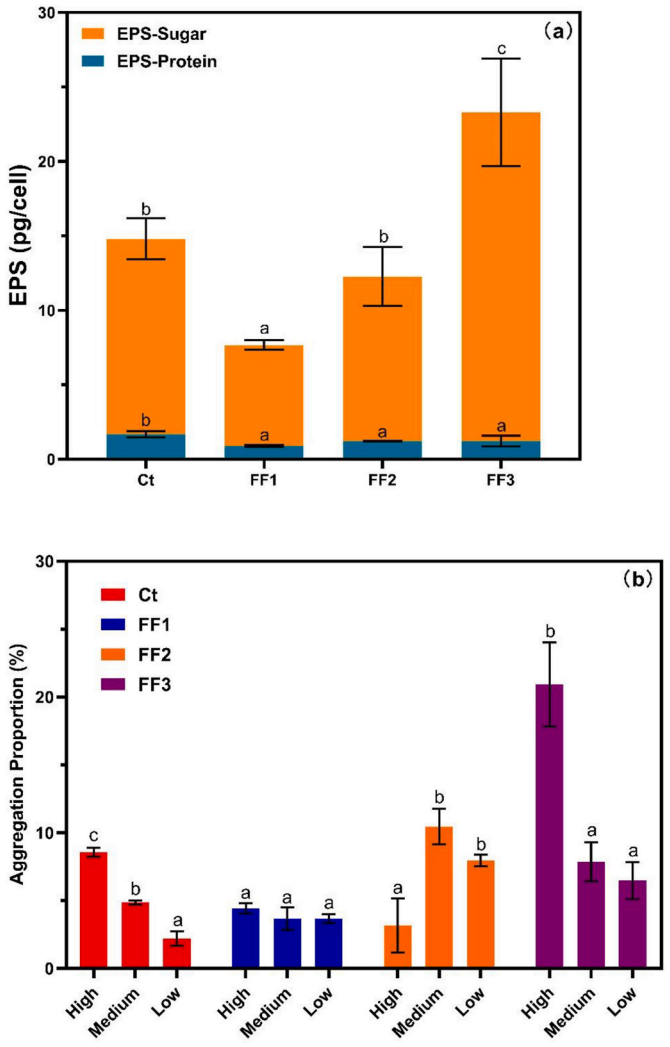

Fig. 6. (a) EPS contents and (b) aggregation proportion of algal cells at different positions in the reactor. Ct: Control, FF1: Wind speed 3 m/s, FF2: Wind speed 6 m/s, FF3: One wave pump (flow rate 0.12 m/s). Data are represented as means ± standard deviation analyzed from three replicates. Different characters indicate significant difference ($P < 0.05$; Tukey's test, followed by Duncan's test).

velocity could affect the growth of cyanobacteria and the trend was similar to the results of this study. Low flow velocity promoted algal growth, as the flow velocity increased, the growth rate slowed down gradually (Zhou et al., 2016a, 2016b). In this study, the flow velocity of FF2 was about 50% higher than the flow velocity of FF1, which may lead to a slower growth rate of algal cells.

4.2. Effects of fluid fields on algal buoyancy

Under different fluid fields, the buoyancy of cyanobacteria has also changed. According to the results of spatial distribution (Fig. 4), algal cells in the control were mainly concentrated at the bottom of the reactor. In the FF1 group, the cell density in the upper part was slightly higher than that in the middle and lower part, on the contrary, algal cells were mostly concentrated in the middle and lower part of the reactor in the FF2 group. The spatial distribution in the FF3 group was similar with the FF1 group, and a clear floating layer of cyanobacteria was observed.

The buoyancy of cyanobacteria is mainly derived from the intracellular gas vesicles and the colonies formed between algal cells (Reynolds et al., 1987). In order to analyze the effects of fluid fields on the synthesis of gas vesicles, relative quantitative analysis of four related genes (*gvpC*, *gvpG*, *gvpJ*, and *gvpK*) was conducted by quantitative real-time PCR. The results showed that compared with the control, the expression of related genes in the FF1 group and the FF3 group was significantly up-regulated, while the FF2 group was down-regulated, indicating that low wind speed or high flow rate can promote the gas vesicles synthesis, and high wind speed was unfavorable to the formation of gas vesicles. Previous study of algae gene expression in different seasons in Lake Taihu found that *gvpC* and other genes related to gas vesicles synthesis were significantly up-regulated during cyanobacterial blooms in summer (Tang et al., 2018). The average wind speed of Lake Taihu in summer is about 3 m/s (Yu et al., 2019), which matched well with the results of this study.

The fluid field has a crucial impact on the formation of cyanobacterial colony as well. Quantitative real-time PCR analysis of *rfbB* gene and *cpsF* gene related to EPS synthesis and transport indicated that there was no notable difference between the control and the FF2 group, meanwhile, related genes were down-regulated in the FF1 group, and up-regulated the FF3 group. Comparing with the total EPS content of each group (Fig. 6a), it was found that the trend was similar to the changes of gene expression. Algal cells can secrete EPS to resist the stimulation or damage of external conditions (Xiao et al., 2018). In this study, algal cells were damaged due to the high shear stress in the FF3 group, which induced the secretion of more EPS to resist the stimulation. No significant damage of algal cells was observed in the FF1 and FF2 group, therefore, their EPS contents were lower than the FF3 group. Besides, the trend of EPS content was also consistent with the antioxidant indicators of each group, which mutually supported the above conclusions.

The increase of EPS content will promote the formation of colony, and the colony structure can provide more buoyancy of algal cells to form the cyanobacterial blooms. Aggregation proportion of algal cells was detected to characterize the colony formation (Fig. 6b). The FF3 group with the highest EPS contents also had the highest aggregation proportion. Meanwhile, comparing the aggregation proportion in different positions of the FF3 group, it was found that the aggregation proportion of the upper part was higher than that of the other parts, which corresponds to the highest proportion of algal cells in the upper layer (Fig. 4d), and suggested that the formation of colony was beneficial to the floating of cyanobacteria.

4.3. Effects of fluid fields on the formation of cyanobacterial blooms

The fluid fields formed under different external conditions were accurately measured by PIV system (Fig. 1). For the wind speed of 3 m/s (the FF1 group), the direction of the flow velocity in the reactor was upward. When the wind speed increased to 6 m/s (the FF2 group), the direction of flow velocity changed to downward. Thus, it can be inferred that the wind speed of 3 m/s is beneficial to the formation of cyanobacterial blooms, while the wind speed of 6 m/s is adverse. Numerous field studies have obtained similar results (Ulrike et al., 2016; Wang et al., 2011; Zhou et al., 2016a). Data analysis of a cyanobacterial bloom formed in Lake Taihu pointed out that for the wind speed of 4–5 m/s, the area of cyanobacterial bloom was only 25 km^2. When the wind speed decreased to 2–3 m/s, the area increased rapidly to 936 km^2. Subsequently, the wind speed increased again to 4–5 m/s and the area drops to 120 km^2 (Wang et al., 2011). In the past 20 years, the frequency of Lake Taihu under breeze (wind speed < 3 m/s) increased from 36.1% to 56.8%, while the frequency of strong winds (wind speed > 6 m/s) decreased from 21.9% to 8.7%. The slowing wind speeds year by year are beneficial to the formation of cyanobacterial blooms (Wu et al., 2015). Under the condition of breeze, divergent air fields can be formed, which further promotes the formation of cyanobacterial blooms (Wang et al., 2010). When wind speed increase to 6–8 m/s, the accumulation of cyanobacterial blooms on the water surface will be broken (Qin et al., 2018).

Different fluid fields led to changes in the shear stress (Figs. S5–S8),

especially the boundary shear stress at the edge of the reactor, whose value was much higher than the shear stress in other areas of the reactor. Researches concerning natural fluid field modeling found that the shear stress is mainly affected by the topography, and the boundary shear stress near the shore is generally greater than the shear stress far away from the shore (Booker et al., 2010; Kähler et al., 2006). In this study, high shear stress was revealed to promote the synthesis of gas vesicles and the formation of colonies, thereby improving the buoyancy of algal cells. These results provide the theoretical basis to explain the phenomenon that cyanobacterial blooms are more likely to form on the lake shore under moderate breeze.

5. Conclusion

The fluid field has an important influence on the formation of cyanobacterial blooms. Low wind speed (3 m/s) is conducive to the formation of cyanobacterial blooms, while high wind speed (6 m/s) is adverse. For the wind speed of 3 m/s, an upward fluid field is formed. This fluid field is not only suitable for the algal growth, but also improves the algal buoyancy by promoting the synthesis of gas vesicle and the formation of colony. In addition, the boundary shear stress can induce the aggregation of cyanobacteria to improve the floating rate, which is beneficial to cyanobacterial blooms formation. As a result, cyanobacterial blooms are more likely to form on the lake shore under moderate breeze. When the wind speed increases to 6 m/s, a downward fluid field is formed, causing algal cells to gather at the bottom, which is not conducive to the formation of cyanobacterial blooms. The results of this study provide a theoretical basis for field researches related to the formation of cyanobacterial blooms. Besides, in China, the algal harvest was widely applied for cyanobacterial blooms control in the past decades (Fan et al., 2019a). The results of this study can be helpful for the prediction of the location where cyanobacterial blooms may occurred, and can be conducive to the deployment of the algal harvest ship and the improvement of efficiency.

Credit author statement

Peng Gu: Conceptualization, Investigation, Data curation, Writing - original draft. Guoping Zhang: Conceptualization, Methodology, Resources. Xin Luo: Investigation, Data curation. Lianghao Xu: Investigation, Data curation. Weizhen Zhang: Methodology, Resources, Software. Qi Li: Methodology, Writing - review & editing. Yuyang Sun: Writing - review & editing. Zheng Zheng: Conceptualization, Supervision.

Declaration of competing interest

The authors declare that they have no known competing financial interests or personal relationships that could have appeared to influence the work reported in this paper.

Acknowledgments

The study was supported by ABA Chemicals, Chengdu University of Technology Research Startup Fund (10912-KYQD2020-08431) for funding support, and we appreciate the technical assistance of Hanqi Wu from Hohai University.

Appendix A. Supplementary data

Supplementary data to this article can be found online at https://doi.org/10.1016/j.chemosphere.2021.131219.

References

Acuña, V., Vilches, C., Giorgi, A., 2011. As productive and slow as a stream can be—the metabolism of a Pampean stream. J. North Am. Benthol. Soc. 30 (1), 71–83.

Baptista, M.S., Vasconcelos, M.T., 2006. Cyanobacteria metal interactions: requirements, toxicity, and ecological implications. Crit. Rev. Microbiol. 32 (3), 127–137.

Booker, D.J., Sear, D.A., Payne, A.J., 2010. Modelling three dimensional flow structures and patterns of boundary shear stress in a natural pool-riffle sequence. Earth Surf. Process. Landforms 26 (5), 553–576.

Bowen, C.C., Jensen, T.E., 1965. Blue-green algae: fine structure of the gas vacuoles. Science 147 (3664), 1460–1462.

Chen, M., Tian, L.L., Ren, C.Y., Xu, C.Y., Wang, Y.Y., Li, L., 2019. Extracellular polysaccharide synthesis in a bloom-forming strain of Microcystis aeruginosa: implications for colonization and buoyancy. Sci. Rep. 9 (1), 1251–1262.

Dubois, M., Gilles, K.A., Hamilton, J.K., Rebers, P.A., Smith, F., 1956. Colorimetric method for determination of sugars and related substances. Anal. Chem. 28 (3), 350–356.

Fan, F., Shi, X., Zhang, M., Liu, C., Chen, K., 2019a. Comparison of algal harvest and hydrogen peroxide treatment in mitigating cyanobacterial blooms via an in situ mesocosm experiment. Sci. Total Environ. 694, 133721.

Fan, H., Liu, H., Dong, Y., Chen, C., Wang, Z., Guo, J., Du, S., 2019b. Growth inhibition and oxidative stress caused by four ionic liquids in Scenedesmus obliquus: role of cations and anions. Sci. Total Environ. 651 (Pt 1), 570–579.

Gu, P., Li, Q., Zhang, W., Zheng, Z., Luo, X., 2020. Effects of different metal ions (Ca, Cu, Pb, Cd) on formation of cyanobacterial blooms. Ecotoxicol. Environ. Saf. 189 (Feb.), 109976.

Huisman, J., Codd, G.A., Paerl, H.W., Ibelings, B.W., Verspagen, J.M.H., Visser, P.M., 2018. Cyanobacterial blooms. Nat. Rev. Microbiol. 16 (8), 471–483.

Imai, H., Chang, K.-H., Kusaba, M., Nakano, S.-i., 2008. Temperature-dependent dominance of Microcystis (Cyanophyceae) species: M. aeruginosa and M. wesenbergii. J. Plankton Res. 31 (2), 171–178.

Jiang, M., Zheng, Z., 2018. Effects of multiple environmental factors on the growth and extracellular organic matter production of Microcystis aeruginosa: a central composite design response surface model. Environ. Sci. Pollut. Res. Int. 25 (23), 23276–23285.

Kähler, C.J., Scholz, U., Ortmanns, J., 2006. Wall-shear-stress and near-wall turbulence measurements up to single pixel resolution by means of long-distance micro-PIV. Exp. Fluid 41 (2), 327–341.

Krüger, G.H.J., Eloff, J.N., 2010. The influence of light intensity on the growth of different Microcystis isolates. J. Limnol. Soc. South. Afr. 3 (1), 21–25.

Lajwant, K.R., Fernando, S.S., Peter, R., 1991. High level expression and purification of dThymidine diphospho-D-glucose 4,6-dehydratase (rfbB) from Salmonella serovar typhimurium LT2. Biochem. Biophys. Res. Commun. 174 (2), 846–852.

Li, Q., Gu, P., Ji, X., Li, H., Zhang, J., Zheng, Z., 2020. Response of submerged macrophytes and periphyton biofilm to water flow in eutrophic environment: plant structural, physicochemical and microbial properties. Ecotoxicol. Environ. Saf. 189, 109990.

Liang, P., Wang, X., Ma, F., 2013. Effect of hydrodynamic conditions on water eutrophication: a review. J. Lake Sci. 25 (4), 455–462.

Liu, F., Liu, Z., Wang, L., Shi, Q., Zhou, J., 2006. On the measurement of velocities and stress in vortex wave field with particle image velocimetry. J. Exp. Mech. 21 (3), 279–284.

Mitrovic, S.M., Hardwick, L., Dorani, F., 2011. Use of flow management to mitigate cyanobacterial blooms in the Lower Darling River, Australia. J. Plankton Res. 33 (2), 229–241.

Phélippé, M., Gonçalves, O., Thouand, G., Cogne, G., Laroche, C., 2019. Characterization of the polysaccharides chemical diversity of the cyanobacteria Arthrospira platensis. Algal Research 38, 101426.

Pratik, K., Krishnamoorthy, H., Satinder, K., Brar, M., Cledon, A., 2018. Biodegradation of microcystin-LR using acclimatized bacteria isolated from different units of the drinking water treatment plant. Environ. Pollut. 242, 407–416.

Qin, B., Yang, G., Ma, J., Deng, J., Li, W., Wu, T., Liu, L., Gao, G., Zhu, G., Zhang, Y., 2016. Dynamics of variability and mechanism of harmful cyanobacteria bloom in Lake Taihu, China. Chin. Sci. Bull. 61, 759–770.

Qin, B., Yang, G., Ma, J., Wu, T., Li, W., Liu, L., Deng, J., Zhou, J., 2018. Spatiotemporal changes of cyanobacterial bloom in large shallow eutrophic Lake Taihu, China. Front. Microbiol. 9, 451.

Qin, B., Zhu, G., Gao, G., Zhang, Y., Li, W., Paerl, H.W., Carmichael, W.W., 2010. A drinking water crisis in Lake Taihu, China: linkage to climatic variability and lake management. Environ. Manag. 45 (1), 105–112.

Reynolds, C.S., Oliver, R.L., Walsby, A.E., 1987. Cyanobacterial dominance: the role of buoyancy regulation in dynamic lake environments. N. Z. J. Mar. Freshw. Res. 21 (3), 379–390.

Rippka, R., Deruelles, J., Waterbury, J.B., Herdman, M., Stanier, R.Y., 1979. Generic assignments, strain histories and properties of pure cultures of cyanobacteria. J. Gen. Microbiol. 111 (6), 1–61.

Schmittgen, T.D., Livak, K.J., 2008. Analyzing real-time PCR data by the comparative C (T) method. Nat. Protoc. 3 (6), 1101–1108.

Smith, P.K., Krohn, R.I., Hermanson, G.T., Mallia, A.K., Gartner, F.H., Provenzano, M.D., Fujimoto, E.K., Goeke, N.M., Olson, B.J., Klenk, D.C., 1985. Measurement of protein using bicinchoninic acid. Anal. Biochem. 150 (1), 76–85.

Tang, X., Krausfeldt, L.E., Shao, K., LeCleir, G.R., Stough, J.M.A., Gao, G., Boyer, G.L., Zhang, Y., Paerl, H.W., Qin, B., 2018. Seasonal gene expression and the ecophysiological implications of toxic Microcystis aeruginosa blooms in Lake Taihu. Environ. Sci. Technol. 52 (19), 11049–11059.

Thurlow, L.R., Thomas, V.C., Hancock, L.E., 2009. Capsular polysaccharide production in Enterococcus faecalis and contribution of CpsF to capsule serospecificity. J. Bacteriol. 191 (20), 6203–6210.

Ulrike, K., Georgiy, K., Brian, B., Brigit, P., Nadine, D., Achim, B., 2016. Low-wind summers promote blooms of cyanobacteria in Lake Tiefer See, NE Germany. In: Egu General Assembly Conference.

Wang, C., Chen, L., Pan, W., Qian, X., 2010. Divergence characteristics and formation mechanism of wind field appropriate for the cyanobacteria bloom in Taihu Lake. China Environ. Sci. 30 (9), 1168–1176.

Wang, W., Zeng, M., Ren, J., 2011. Numerical study of the impact of surface wind changes on the cyanobacteria bloom in Lake Taihu. Journal of the Meteorological Sciences 31 (6), 718–725.

Wu, T., Qin, B., Justin, D.B., Shi, K., Zhu, G., Zhu, M., Yan, W., Wang, Z., 2015. The influence of changes in wind patterns on the areal extension of surface cyanobacterial blooms in a large shallow lake in China. Sci. Total Environ. 518–519, 24–30.

Xiao, M., Li, M., Reynolds, C.S., 2018. Colony formation in the cyanobacterium Microcystis. Biol. Rev. 93 (3), 1399–1420.

Xu, H., Paerl, H.W., Qin, B., Zhu, G., Hall, N.S., Wu, Y., 2015. Determining critical nutrient thresholds needed to control harmful cyanobacterial blooms in eutrophic Lake Taihu, China. Environ. Sci. Technol. 49 (2), 1051–1059.

Yang, Z., Kong, F., Shi, X., Zhang, M., Cao, H., 2010. Changes in the morphology and polysaccharide content of Microcystis aeruginosa (Cyanobacteria) during flagellate grazing. J. Phycol. 44 (3), 716–720.

Yu, M., Hong, G., Zhu, G., Quan, Q., Xu, H., Zhu, M., Ding, W., Li, W., Wu, T., 2019. Wind field influences on the spatial distribution of cyanobacterial blooms and nutrients in meiliang bay of Lake Taihu, China. Environ. Sci. 40 (8), 3520–3529.

Zhang, Y., Li, H., Kong, F., Yu, Y., Zhang, M., 2011. Role of conony intercellular space in the cyanobacteria bloom-forming. Environ. Sci. 32 (6), 1602–1607.

Zheng, X., Yuan, Y., Li, Y., Liu, X., Fan, Z., 2020. Polystyrene nanoplastics affect growth and microcystin production of Microcystis aeruginosa. Environ. Sci. Pollut. Control Ser. 28 (11), 1–10.

Zhou, J., Qin, B., Han, X., 2016a. Effects of the magnitude and persistence of turbulence on phytoplankton in Lake Taihu during a summer cyanobacterial bloom. Aquat. Ecol. 50 (2), 197–208.

Zhou, J., Qin, B., Han, X., Zhu, L., 2016b. Turbulence increases the risk of microcystin exposure in a eutrophic lake (Lake Taihu) during cyanobacterial bloom periods. Harmful Algae 55, 213–220.

Zhu, G., Qin, B., Gao, G., 2004. Vertical distribution of the concentrations of phosphorus and suspended solid in Taihu lake affected by wind-induced wave. Adv. Water Sci. 15 (6), 776–780.